

On the Performance of Concept Probing: The Influence of the Data

– Extended Version –¹

Manuel de Sousa Ribeiro, Afonso Leote and João Leite

NOVA LINC, NOVA School of Science and Technology, NOVA University Lisbon, Portugal
{mad.ribeiro, a.leote, jleite}@fct.unl.pt

Abstract. Concept probing has recently garnered increasing interest as a way to help interpret artificial neural networks, dealing both with their typically large size and their subsymbolic nature, which ultimately renders them unfeasible for direct human interpretation. Concept probing works by training additional classifiers to map the internal representations of a model into human-defined concepts of interest, thus allowing humans to peek inside artificial neural networks. Research on concept probing has mainly focused on the model being probed or the probing model itself, paying limited attention to the data required to train such probing models. In this paper, we address this gap. Focusing on concept probing in the context of image classification tasks, we investigate the effect of the data used to train probing models on their performance. We also make available concept labels for two widely used datasets.

1 Introduction

In this paper, we investigate how different characteristics of the data required for concept probing in neural network models - such as size, number of features, provenance, and quality - affect the performance of popular concept probing methods.

The application of neural networks in tasks that may influence the health or safety of individuals highlights the urgency for methods to interpret neural network models and validate how they achieve their results [59]. The field of Explainable AI seeks to address this issue, providing methods to help improve a model’s interpretability.

One of the most prominent methodologies for interpreting neural network models is known as *concept probing* [2]. Concept probing consists of training a model – referred to as *probe* – to identify a given concept of interest from the activations of an existing neural network model. In this way, one is able to estimate the mutual information between the representations of a model and some concept of interest [38], with higher prediction accuracy implying that the representations carry more information about the concept of interest. Concept probing provides some insight into what is encoded in the representations of a neural network model without the need to retrain or modify the model being examined. It allows humans to define and experiment with their own concepts of interest according to their needs and requirements.

Apart from providing humans with a way to *peek* into what is encoded within a neural network model, the trained probes can be used

to map subsymbolic internal representations of a model into symbolic observations regarding a model’s internal state. These probes can then be leveraged by interpretability and explainability methods, e.g., to test the behavior of a model’s internal representations [33], to produce human-understandable justifications for a neural network’s output [13, 16], or to generate and study a model’s counterfactual behavior [55], to name a few.

This methodology has sparked interest in different communities, which have mainly focused on matters regarding the design of the probing models and the interpretation of their results. However, as stressed in [4], matters regarding the data that is necessary to properly develop concept probes have been largely overlooked. In the absence of such studies, practitioners have to rely on their intuitions, which often leads to the widespread of unproven *folk theories* concerning crucial issues on concept probing. Questions such as “How much data does concept probing require?”, “Can concept probing handle large models?”, “Does one need a *fresh* dataset for concept probing? Or can one repurpose the data used in the development of the probed model?”, and “Does concept probing require high-quality data?” have long been asked in the community, with their answers often taken for granted without dedicated studies supporting them. This has significant repercussions on the research being carried out. E.g., [36] describes using vast amounts of data for probing because the number of required samples is unclear. This is a significant issue as data is generally the major cost of employing concept probing, since labeled data is necessary to probe for each concept of interest. It is thus essential to have a clearer understanding of how the data used to train probing models affects their performance, as it will allow practitioners to better assess when it is feasible to apply concept probing and how to do it effectively – understanding the existing trade-offs and avoiding common pitfalls, like using an inadequate amount of training samples or neglecting to assess their data’s quality.

In this paper, we focus on some of the most common yet scarcely addressed questions about how the characteristics of the datasets used to train such probing models might affect their performance. Based on a representative selection of image classification datasets, neural network models, and probing architectures from the literature, we perform a thorough experimental evaluation of the influence of data in concept probing along four main dimensions, namely: i) testing the effect of the probing models’ train data size on their performance; ii) inspecting how the size of the probed model impacts the probing model’s performance; iii) examining the impact of reusing

¹ This is an extended version of [10].

data from the probed model train set to train the probing models; iv) verifying how the quality of the probing models’ training data affects their performance. While doing so, we also examine the behavior of the most popular probing architectures on various image classification neural network models and datasets.

Our results confirm some existing ideas on the influence of data in concept probing but also support some surprising conclusions related, e.g., to data reuse and the robustness of probing models, that ultimately impact probing’s applicability.

The remainder of this paper is organized as follows: Section 2 offers an overview of concept probing, followed by a description of the methods and experimental setup in Section 3. Then, in Section 4 through 7, we present and discuss our experimental results. Finally, we discuss some related work in Section 8 and conclude with a summary of our findings in Section 9.

2 Concept Probing

The intuition behind concept probing is that neural networks distill useful representations over the course of their layers, which allow them to gradually abstract away from the input space and can finally be used to produce their expected outputs. Thus, one could monitor such representations by observing the activations of a model’s units and assess how well they represent some given concept of interest – also referred to as *property* in the literature [4].

Hence, in concept probing, a given neural network model $f: x \mapsto y$ – which we refer to as *original model* – is probed for representations with information regarding some human-defined concept of interest C . The way the probing occurs is by mapping the internal representations of f to C by means of another model g – referred to as *probe*. Typically, probes do not map all internal representations of some original model f , but a subset of those. E.g., the activations produced by all units of a given layer of the model f . Let $f_u(x)$ denote the representation of x at some sequence of units u from model f , i.e., the activations generated by model f when fed with input x at units u . A probing model $g: f_u(x) \mapsto c$ is a model trained to identify some concept of interest C , with c representing its value, from some internal representations u of the original model f . As an example, f might be a convolutional neural network trained to classify a bird’s species from an image, and g might be a classifier mapping the output of the convolutional part of f to some concept of interest C , such as whether a bird’s *yellow belly* is visible in the image – a concept which is relevant to identify some bird species.

The dataset to train a probe model g is different from the one used to train f , $\mathcal{D}_f = \{x^{(i)}, y^{(i)}\}$, which is composed of input samples x of f and their respective outputs. The probe’s dataset should be composed of the observed activations of f for a set of instances, along with annotations for the corresponding value of the concept of interest C for that instance, i.e., $\mathcal{D}_g = \{f_u(x^{(i)}), c^{(i)}\}$. This dataset is generally balanced wrt. the concept values ($c^{(i)}$). The semantics of concept of interest C is given extensionally by the dataset \mathcal{D}_g .

The performance of g is measured after its training on a separate test dataset \mathcal{D}'_g , similar to \mathcal{D}_g but made of fresh instances. Since the data is typically balanced, the accuracy of g on \mathcal{D}'_g is generally considered, with higher accuracies indicating that the units u probed by g carry more information for representing concept C . Throughout our experiments, we discuss how different characteristics of the dataset \mathcal{D}_g might affect the performance of a probing model g .

The particular architecture of a probing model is still a debated issue, with some works advising the use of simpler linear probing models [2, 31], while others suggest that more complex probing ar-

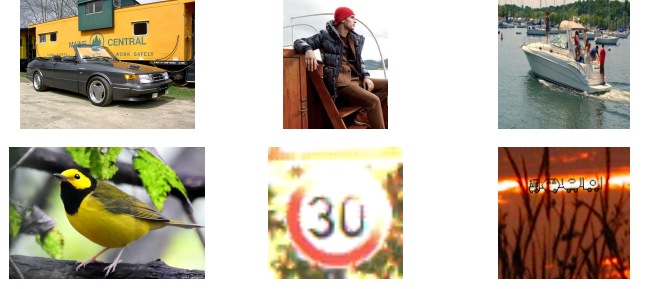


Figure 1. Sample images from each dataset: ImageNet [14], DeepFashion [32], Places365 [64], CUB [58], GTSRB [51], and XTRAINS [8].

chitectures should be considered [37, 38, 55]. In this work, we consider both types of probing architectures.

3 Methods and Experimental Setup

To study how various characteristics of the data used for concept probing influence the resulting probes, one should consider various datasets, original models, and probing architectures. In this section, we describe the probing models’ architectures used in our empirical study. Subsequently, we introduce the datasets used in the experiments and their respective original models.

3.1 Probing Architectures

We consider five different architectures for probe g – a linear logistic regression classifier (Logistic); a linear ridge classifier (Ridge); a LightGBM decision tree (LGBM) [24]; a neural network (NN); and a mapping network probe (MapNN) [13] – ensuring that our results are not too tied to a particular kind of probe. When training all models, 25% of the training data was used as a validation set. If early stopping is used, we consider a patience value of 15. For the linear Ridge probe, we perform a hyperparameter search over the alpha values of [0.01, 0.05, 0.1, 0.5, 1, 5, 10, 50, 100]. The LGBM probe is used with default parameters, except for the minimal number of instances at a terminal node, which is reduced when the default value is too large for the model to train. The validation set is used together with early stopping to select the number of boosting rounds. The NN probe has a feedforward architecture with ReLU non-linearity and a hidden layer of size 10. The MapNN probe shares the same architecture as the NN, but L1 regularization is applied to its weights with a strength of 0.001. Mapping network probes are trained using the input reduce procedure described in [13], a procedure that iterates a set of layers of a model to identify a subset of units from which some concept of interest might be probed from, with a patience value of 3 and the ranking of each feature being given by its maximum absolute weight. Early stopping is used to select the number of training epochs for both the neural network and the mapping network probes.

All probes are trained using the activations produced by some given layer of an original model f , with the exception of the mapping network probes, which use the input reduce procedure, and thus might select units u from various layers of the original model f .

3.2 Datasets and Original Models

We experiment with probing eight trained neural network models, from six image classification datasets. Table 1 presents a summary of the experimental setting for each dataset. These datasets are representative of a variety of different image classification settings where

Property	ImageNet	DeepFashion	Places365	CUB	GTSRB	XTRAINS _{A;B;C}
Type	Real	Real	Real	Real	Real	Synthetic
Task	Multiclass	Multiclass	Multiclass	Multiclass	Multiclass	Binary
# Class	1000	12	365	200	43	1; 1; 1
Image Entropy	0.91	0.74	0.93	0.89	0.79	0.76
Compression Ratio	1.09	1.05	1.08	1.11	2.44	2.00
Concept Separability	0.59	0.58	0.63	0.63	0.84	0.52
Original Model	ViT	ResNet101	ResNet50	ResNet50	MobileNetV2	VGGNet
Pre-trained	Yes	Yes	Yes	Yes	No	No
Input Shape	224 × 224 × 3	224 × 224 × 3	224 × 224 × 3	224 × 224 × 3	128 × 128 × 3	152 × 152 × 3
Model Size (# params)	85.8 M	44.5 M	28.4 M	28.4 M	2.3 M	421; 421; 561 K

Table 1. Experimental setting of each dataset.

concept probing might be applied, ranging from binary classification to multiclass classification with 1000 classes. The image complexity of the datasets, measured by their *entropy* and *compression ratio* [62], reveals a set of settings with moderately and highly complex images. In some cases, the probed concepts are closer to the images, indicated by a high concept separability score – measured as the accuracy of a linear model predicting the concepts from the images – while in others, the concepts are more abstract. Simultaneously, both simpler and more complex original models are considered, illustrating different circumstances for the application of concept probing.

ImageNet [14]: this dataset has labels for 1000 varied object classes. As the original model, we consider the Vision Transformer (ViT) from [61] with 84.2% accuracy on the test set, which we refer to as $f_{ImageNet}$. We probe 11 random concepts from the related ImageNet Object Attributes dataset [42], a subset of ImageNet with labels for attributes related to colors, shapes and textures: $\exists hasTexture.Furry$, $\exists hasColor.Green$, $\exists hasShape.Rectangular$, $\exists hasColor.Red$, $\exists hasShape.Round$, $\exists hasTexture.Shiny$, $\exists hasPattern.Spotted$, $\exists hasPattern.Striped$, $\exists hasTexture.Wet$, $\exists hasTexture.Wooden$, and $\exists hasColor.Yellow$.

DeepFashion [32]: this dataset contains images of 50 different clothes categories, with 1000 different labeled clothing-related attributes. It is known to be highly imbalanced and noisily labeled [50]. As the original model, we consider a ResNet101 pre-trained in ImageNet [14] and finetuned to classify the 12 most populated clothes categories in this dataset, achieving a test accuracy of 59.60% in a balanced test set of 16 800 images. We refer to this model as $f_{Fashion}$. From this dataset, we probe the following 11 clothing-related attributes: $Bodycon$, $\exists has.FauxLeather$, $\exists has.Graphic$, $\exists has.Hooded$, $Maxi$, $Midi$, $Moto$, $Pencil$, $\exists has.Racerback$, $Skater$, and $\exists has.Strapless$.

Places365 [64]: this dataset is composed of images of 365 scene categories. As the original model, we consider the ResNet50 from [64] trained to classify each scene category with a test accuracy of 54.65%, which we refer to as f_{Places} . As this dataset has no additional annotations, we probe the 10 concepts defined in the CIFAR-10 dataset [27]: $Airplane$, $Automobile$, $Bird$, Cat , $Deer$, Dog , $Frog$, $Horse$, $Ship$, and $Truck$.

Caltech-UCSD Birds-200-2011 (CUB) [58]: this dataset has images of birds from 200 species. Each image is labeled with various attributes representing visual concepts that are described as relevant to the identification of the bird species. From these attributes, we randomly selected the following 11 concepts to probe: $\exists hasBillShape.Needle$, $\exists hasBillShape.HookedSeabird$, $\exists hasHeadPattern.Striped$, $\exists hasBreastColor.Yellow$, $\exists hasThroatColor.Red$, $\exists hasEyeColor.Red$, $\exists hasBellyColor.Blue$, $\exists hasBellyColor.Yellow$, $\exists hasShape.DuckLike$, $\exists hasCrownColor.White$, $\exists hasCrownColor.Red$. As the original model, we consider the

ResNet50 from [53] pre-trained in the iNaturalist dataset [20] and finetuned in the CUB dataset, achieving an accuracy of about 85.83% on the dataset’s test data. We refer to this model as f_{CUB} .

As observed in [63, 26], CUB’s attributes are noisily labeled. We relabeled a subset of the data for each of the probed concepts², which we use in our experiments. We further discuss this topic in Section 7.

German Traffic Sign Recognition Benchmark (GTSRB) [51]: this dataset has images of 43 types of traffic signs. Additionally, we consider an ontology and labels based on the 1968 Convention on Road Signs and Signals [56], which describes each type of traffic sign in the dataset based on visual concepts³. For example, a stop sign is described as having an octagonal shape, a red ground color, and a white ‘stop’ symbol. We probe the following 10 random concepts defined in the ontology: $\exists hasSymbol.T$, $\exists hasBar.Black$, $\exists hasSymbol.Black$, $Blue$, $\exists hasShape.Circular$, $Pole$, $\exists hasGround.Red$, $\exists hasSymbol.Speed80$, $\exists hasShape.Triangular$, and $\exists hasGround.White$. As the original model, we trained a MobileNetV2 [43] – which we refer to as f_{GTSRB} – to identify the class of the traffic sign in an image, achieving an accuracy of about 98% on the dataset’s test data.

Explainable Abstract Trains Dataset (XTRAINS) [8]: this synthetic dataset contains representations of trains over landscape backgrounds. It is accompanied by an ontology describing how different concepts in the dataset relate to each other, with each concept having its own visual characteristics. Three different types of trains (TypeA, TypeB, and TypeC) are defined based on these concepts. E.g., the concept of $PassengerCar$ is visually represented by a wagon having at least one circle inside of it, with the dataset’s ontology stating that trains having at least two passenger cars are $PassengerTrains$, and that such trains are TypeB trains. The dataset provides labels for all of these concepts. As original models, we consider the three VGGNet [49] models from [16] – referred to as f_A , f_B , and f_C – trained to identify trains of the corresponding type, each achieving a test accuracy of about 99%. We probe the 11 concepts examined in [13]: $EmptyTrain$, $FreightTrain$, $\exists has.FreightWagon$, $LongTrain$, $\exists has.LongWagon$, $MixedTrain$, $\exists has.OpenRoofCar$, $PassengerTrain$, $\exists has.ReinforcedCar$, $RuralTrain$, and $WarTrain$.

Probed Activations To avoid having our results too tied to the choice of probing the activations of a particular layer of a model, we considered the activations produced by a set of representative layers for each model, taking into account the model’s architecture and concepts that were being probed.

For the VGGNet models (f_A , f_B , f_C), which have a clear separation between convolutional and dense parts, we probe the activations resulting from their convolutional part and each hidden dense layer. For the MobileNetV2 model (f_{GTSRB}), which is composed of 17

² Details are made available in Appendix A.

³ Details are made available in Appendix B.

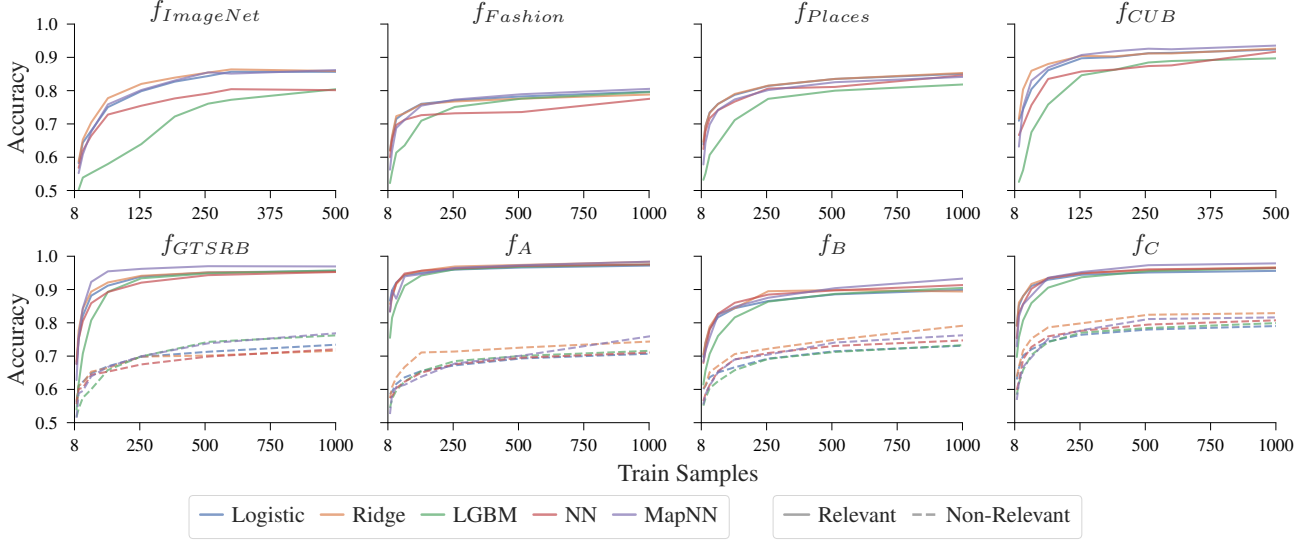


Figure 2. Probe performance by amount of training data.

residual layers, we consider the activations of every fourth residual layer. For the ResNet50 (f_{Places} , f_{CUB}) and ResNet101 ($f_{Fashion}$) models, which are composed of 4 residual blocks, we probe the activations produced by the first and last convolution blocks of the fourth residual block, as the activations resulting from the previous blocks seemed to not yet capture the probed concepts. Similarly, for the ViT model ($f_{ImageNet}$), we consider the activations resulting from the attention and feedforward layers of the model’s last transformer block.

Concept Relevancy In our experiments, we distinguish between two sets of probed concepts: relevant and non-relevant. Informally, a concept is said to be relevant to another if there is any circumstance where knowledge relative to the former allows us to infer knowledge about the latter. E.g., consider f_{CUB} , which identifies bird species in CUB. All Hooded warbler birds have a yellow belly; thus, yellow belly is a relevant concept to Hooded warbler birds, as knowing about it might allow us to infer whether a bird is a Hooded warbler. [13] provides a more formal definition of relevancy for concepts defined through ontologies in Description Logics, which we use to determine relevant concepts in the setting of the GTSRB and XTRAINS datasets. For the CUB dataset, although no ontology is provided, [58] states that the attributes were selected based on an expert’s guide on identifying birds, and thus all concepts are considered to be relevant. Similarly, while no ontology is provided for the ImageNet, DeepFashion, and Places365 datasets, we believe the probed concepts are relevant – at least in the informal sense – to the task being performed by the respective original models.

While being a relevant concept does not provide guarantees concerning concept probing, since a model might learn to perform its task in a way that does not follow our human ontology of a domain, we nevertheless expect that, on average, probing for relevant concepts should yield better results than probing for non-relevant ones.

Methodological Considerations All experimental results in this paper are averaged over 5 repetitions, using different balanced sets of samples for training, validation, and testing. Due to the variance in the amount of available data in each dataset, we test the trained probes with balanced sets of 1 000 test samples for the Places365 and XTRAINS datasets, 200 for DeepFashion and GTSRB, and 100 for the ImageNet and CUB datasets. Except for Section 4, where the

effect of train data size is discussed, all probes were trained using a balanced set of 500 samples. For some concepts in the ImageNet and CUB datasets, there was insufficient data to produce a balanced set of 500 samples, so the nearest balanced amount was considered.

4 Effect of Train Dataset Size

Perhaps the first and most prevalent question when discussing the feasibility of concept probing is, “How much data is necessary?” This is a sensible question to ask, given that for each concept of interest that one aims to probe, a set of labeled data \mathcal{D}_g is required, making data one of the main costs for applying concept probing.

An underlying assumption shared by those working on concept probing is that neural networks distill, throughout their layers, computationally useful representations with information that allows them to address their tasks [2]. Therefore, it is fair to expect that if the concept C being probed is indeed relevant for the task that a neural network f was trained for, then its internal representations have likely distilled some information that is related to C . By leveraging these representations, one should be able to train a probing model g to identify C , even with few train data.

To assess this hypothesis, we train and test a probe g of each considered probing architecture for each original model f , while varying the amount of training data available. Figure 2 shows the average accuracy of each probing architecture over the considered layers for each model f for relevant and non-relevant concepts. In the setting of the ImageNet and CUB datasets, the maximum amount of samples is fewer than in the others due to insufficient sample availability.

The results show that the accuracy of the probes grows quickly for relevant concepts, starting to stabilize at around $|\mathcal{D}_g| = 200$ training samples. Non-relevant concepts seem to require additional training samples while achieving significantly worse results. We attribute these results to the fact that there are fewer incentives for a model to retain information in its inner representations regarding concepts that are not relevant to its task. These results seem to support our conjecture, with the relevant concepts requiring fewer samples than the non-relevant ones.

We also observe that the probes using some kind of regularization – such as the Ridge and MapNN – seem to, on average, achieve better

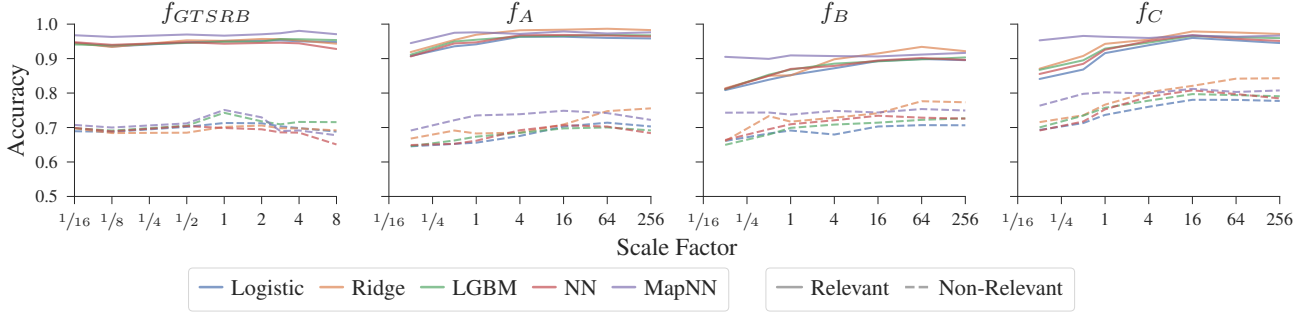


Figure 3. Probe performance by scaling of the original model’s size.

results. Furthermore, in the case of MapNN, a t-test shows that its accuracy is statistically significantly higher than the remaining probes when probing from $f_{ImageNet}$, $f_{Fashion}$, f_{CUB} , f_{GTSRB} , f_A , f_B , and f_C , with the maximum amount of available data. Additionally, Ridge seems to be the probe that is benefiting less from additional data, showing, on average, a smaller accuracy increase from 500 to 1000 samples than all other probe architectures.

These results indicate that one should be able to accurately probe relevant concepts with few training samples – on average, the probe’s performance reaches 97.3% of its maximum measured value with as few as 250 training samples (about 0.8% of the original model’s training data). While the particular values may vary depending on the model being studied and concepts being probed, we consider these results to be encouraging, supporting that concept probing might still be feasible even when the amount of available data is limited.

5 Effect of Original Model Size

Since concept probes are trained based on the activations of a neural network model, as models grow in size, so does the number of their activations, raising the question of how this impacts the training of probes. In this section, we investigate the relationship between the original model’s size and the resulting probe’s performance.

Consider two models f_1 and f_2 , both trained to perform the same task and having achieved a similar test performance, where f_2 is a scaled-up version of f_1 . We hypothesize that if we probe both models using the same probe and data, the probing performance should remain unchanged or slightly deteriorate in f_2 , as the number of probed units increases without necessarily providing new information to help improve the probe’s training, i.e., we expect the added units to mainly provide redundant information.

To test this hypothesis, we need to train multiple original models, scaling up or down their sizes while ensuring that the resulting model’s accuracy was kept similar to the initial (without rescaling) original model. Given the time and computational resources required to train such scaled versions of the original models in settings where large models with pretraining were utilized, these experiments were only conducted in the settings of the XTRAINS and GTSRB datasets. For the models trained in the XTRAINS dataset, the convolutional part of the model was frozen, and only the dense layers were rescaled and retrained. A different approach was taken for the MobileNetV2 architecture, which was used in the setting of the GTSRB dataset, where there is no such separation. The models were retrained from scratch, rescaling the whole network architecture. Only models with a difference smaller than 1.5% in test accuracy from the initial model were considered.

In Figure 3, we show the resulting average probe accuracy for the considered concepts in each dataset while varying the size of the original models. The explored scale factors differ for the GTSRB and XTRAINS datasets due to the large difference in the size of the models used in each setting.

Perhaps surprisingly, we observe that the accuracy of the probing models seems to slightly increase with the scaling up of the original models’ size within the tested scale factors, which generate rather large models. The largest scale factors led, on average, to a 1.8% test accuracy increase. This might be due to the additional features providing some new information that is beneficial for the probing models. Additionally, we observe that scaling down the models seems to deteriorate the probes’ performance, especially for the smaller models used in the XTRAINS dataset, reducing the accuracy by 3.9%. This might indicate that, due to the limited size of the models’ representations, the models had to somehow compress these representations, making the probing of each concept increasingly more complex. A similar observation was made in [36], where they probe from the most compressed layer of an autoencoder, and observe that the probing performance worsens, especially for linear probes. Interestingly, we observe that the mapping network probes seem mostly unaffected by the scaling down of the original model’s size, likely because they are able to select units from various layers.

We conclude that, despite the vast number of features often considered by probing models, they are mostly able to successfully map them to their respective concepts. This is quite relevant because model sizes have been increasing in the last few years [57], indicating that concept probing is still feasible even when dealing with larger-sized models without compromising the probe’s performance.

6 Effect of Reusing Data

When training the probes, it is common practice to use the activations $f_u(x^{(i)})$ generated by samples $x^{(i)}$ that were *not* involved in the training of the original model f , e.g., [36]. This is usually done to avoid any undesirable effects that reusing the same data might have on the probe model’s training. For example, one might hypothesize that the activation patterns of a neural network model f are different for samples used in f ’s training and for samples from the same domain that were not involved in its training. If this were the case, one might expect that by training some probe g on the activations produced by the original model’s f training samples, the resulting probe might underperform when tested on samples that were not involved in f ’s training. In this section, we examine the effect of reusing the same input samples $x^{(i)}$ from the original model’s train set \mathcal{D}_f on the probing model’s train set \mathcal{D}_g .

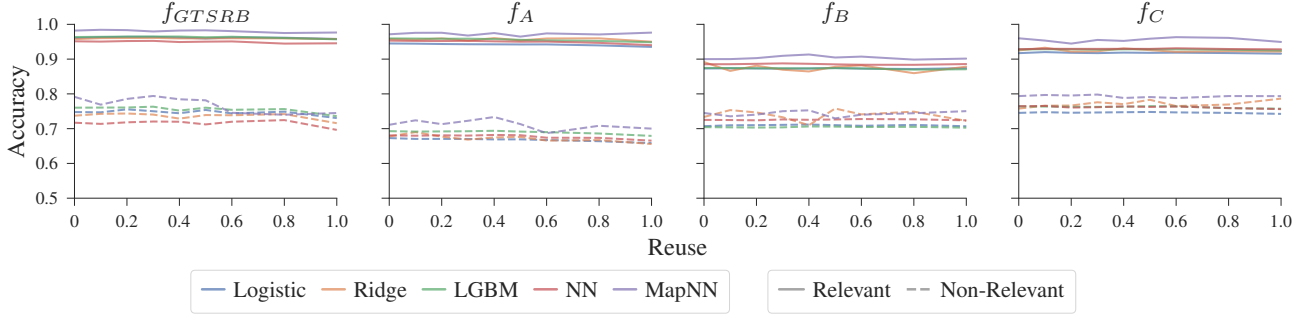


Figure 4. Probe performance by percentage of data reuse from the original model’s training data.

If reusing the input samples $x^{(i)}$ from the original model’s train set \mathcal{D}_f to train some probe model g has some negative impact on the resulting probe’s performance, then we should expect that the test performance of probe g would decrease as the percentage of samples $x^{(i)}$ from the original model’s train set \mathcal{D}_f in the probe’s training set \mathcal{D}_g increases. Otherwise, the resulting performance should remain relatively unchanged.

To test this effect, we need to train multiple probes while varying the amount of reused data from their respective original models’ train set \mathcal{D}_f . Given that $f_{ImageNet}$, $f_{Fashion}$, and f_{CUB} were trained using all available training data and that f_{Places} ’s training data is disjoint from its probe’s training data, we could not reproduce this experiment in these settings, thus focusing on the GTSRB and XTRAINS datasets.

In Figure 4, we show the average performance of the trained probes when varying the amount of reused data. Interestingly, the performance of the trained probes g remains mostly unchanged, even when all of g ’s training data came from their respective original model’s training set. In fact, if we fit a line of best fit to the results, its slope is just slightly negative (-4.1×10^{-3}), with a t-test showing that there is no statistically significant evidence that the amount of reuse affects performance, i.e., that this slope is different from zero.

While we did not observe any significant decrease in the model’s performance when trained with the same data that was used to train its original model, this does not imply that there are no consequences for this decision. Effects of reusing the original model’s training data might manifest in other ways that are not measurable by a probe’s test accuracy. However, this provides us with a helpful insight: – the resulting probe does not seem to overfit to the original model’s activations when trained with reused data, which is one of the main causes of concern on this matter. These results are quite significant for domains where data might be scarce, and thus, being able to reuse the same data that was already gathered for the training of the original model might prove particularly useful.

7 Effect of Data Quality

Data quality is essential for any data-driven approach [45], such as machine learning. However, for a variety of reasons, data quality often falls short of being satisfactory [35]. Given the diagnostic nature of concept probing, where a model is trained to identify some concept of interest given the activations of another model, it is reasonable to inquire how data quality might impact a probe’s performance.

There exist various ways to assess the quality of data [18]. Here, we consider label accuracy, i.e., how accurate are the labels $c^{(i)}$ in a probe’s dataset $\{f_u(x^{(i)}), c^{(i)}\}$. This seems relevant given that con-

cept probing is generally applied on a different set of labels from the ones used to train the original model, which might not always be as carefully considered. The CUB dataset illustrates this situation, where bird species constitute the main labels of the dataset, with the attribute labels being found to be noisy [63].

To examine the effect of varying the quality of a probe’s training data, we artificially introduced noise in the concept labels by inverting the label value of a random subset of the samples. Figure 5 shows the average probe accuracy for each original model while varying the percentage of noisy train samples.

The probing models seem to be robust to a reasonable amount of noise. Introducing 20% of noise in a probe’s train labels led to a relative performance reduction of 9.3% on average. The effect of the introduced noise seems to aggravate significantly when more than 30% noise is added to the train data.

To further validate the effect of the artificially introduced noise and compare it with naturally occurring noise in the samples’ labels, we train and test probes with the original attribute labels provided in the CUB dataset, which are known to be noisily labeled [63]. For the probed concepts in the CUB dataset, we found that 18.2% of the attribute labels were incorrectly specified, with the vast majority of these (93.4%) being samples where a concept was mislabeled as being present. Training with these labels led to a relative performance reduction of 13.1%, which is significantly higher than the one resulting from the artificially introduced noise. This is understandable since the noise in the original CUB labels is not random and mainly affects the positive samples.

While these results are encouraging – suggesting that probes exhibit some robustness to noise in the labels – they should encourage the community to validate the quality of the data used when applying concept probing, and also inspire and motivate, we hope, the development of high-quality benchmarking datasets designed with concept probing research in mind.

8 Related Work

Until recently, the most popular methods to interpret neural network models were saliency and attribution methods [52, 40, 23], which explain a model’s prediction by providing a set of input features and their corresponding contributions, and proxy-based methods [46, 3, 41], which generate an interpretable model with similar behavior to the original one. However, user studies [1, 6, 48] showed that the explanations provided by these methods were often disregarded or unhelpful to end users. This might be attributed to these methods explaining a model’s behavior in terms of its input features, which might not always be meaningful or understandable to users. For example, highlighting a set of pixels from an image to a user

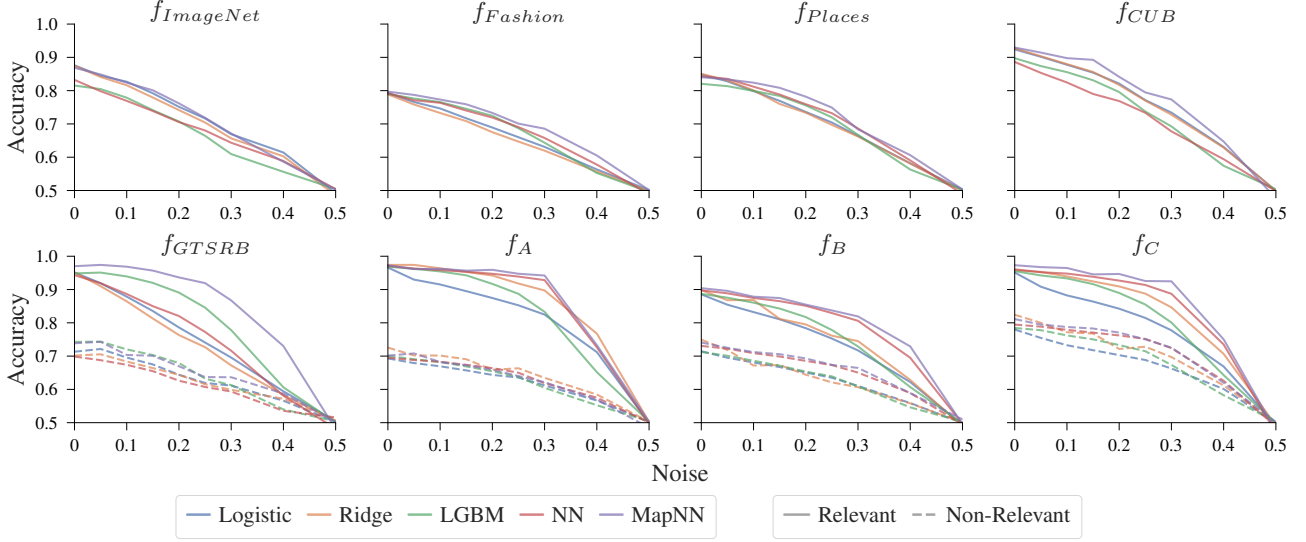


Figure 5. Probe performance by amount of noise in data labels.

does not necessarily convey to the user the meaning of such pixels or how they were used by the model. All of this guesswork still has to be done by the user.

Concept-based explainable AI [39, 28, 47, 29] emerged from the human necessity to interpret models through concepts (symbols) that are relevant and understandable to them, abstracting away from the particular input features of a model. Multiple works have been based on the idea of relating the internal representations of neural network models to human-defined concepts of interest. Some attempt to interpret individual units of a model [34], while others attempt to interpret a layer [25, 7], or even whole models [21].

Concept probing also stemmed from such ideas and became one of the most prevalent frameworks for interpreting neural network models in a concept-based manner. Numerous works have been developed based on concept probing, some focus on examining what it tells us about the model being probed [2, 38], while others focus on the architectures of concept probing models [37, 44, 65], and others investigate concept probing on different kinds of models, such as LSTMs [30] and RNNs [22], or in different domains, like natural language processing [54] and game playing [36]. Others have leveraged concept probing to develop methods to interpret or explain neural networks, e.g., to induce theories describing a model’s internal classification process [16], to test whether a model’s internal representations are consistent with some logic theory [33], or to produce symbolic justifications for a model’s outputs [13].

Despite the growing body of work on concept probing, there is a lack of work on understanding how the data used to train probing models affects the probes’ results, as discussed in [4]. This gap in the literature is significant, as concept probes are often used to assess properties regarding the probed model, and their development is underpinned by their training data. While there exists some work where various datasets and models are probed [11, 19, 5], these do not address the effects that the data has on the probing models, focusing instead on what can be inferred regarding the probed models.

As mentioned in Section 5, the mapping network probes, which use a procedure to select the units from which they probe, kept their probing accuracy even when probing from models with a smaller size. This corroborates the fact that the units used to probe a concept highly influence the resulting probe’s accuracy. [15] describes the use

of elastic-net regularization to identify which units in a layer encode a given concept.

Throughout this work, we have shown that the results of probing for concepts relevant to a given model’s task are substantially different from those of concepts that are not relevant. While the topic of how to identify relevant concepts is outside the scope of this paper, we point out that there exists research aimed at discovering concepts that are relevant for a model’s predictions [21, 17], which might help practitioners identify concepts to probe for.

9 Conclusions

In this paper, we investigated the effect that the data used to train concept probes has on their resulting performance on image classification tasks. To this end, we performed a thorough experimental evaluation with datasets with varied characteristics, using different kinds of probes on neural network models with diverse architectures.

We conclude that concept probing generally requires few train data for concepts that are relevant to the probed model’s task, even – perhaps surprisingly – when probing the representations of large models, which provides additional evidence that probing models are capable of leveraging the knowledge distilled within the probed model’s representations to establish a mapping to their respective concepts. This evidence is further strengthened by the observation that probing models for non-relevant concepts achieve a significantly worse test performance while requiring additional training data.

We also found that repurposing the data involved in the training of the probed model to train probing models does not degrade their resulting test accuracy, providing a valuable insight which suggests that this might be a viable approach in settings where data is limited.

We further conclude that, despite the probing models’ moderate robustness when faced with low-quality data in the form of mislabeled train samples, more effort should be put into assessing the quality of data. This is particularly relevant given the kind of inferences about models that are made based on concept probing, and given that well-known machine learning datasets often have low quality [35].

Our experiments can also be used to compare the behavior of the most popular probing architectures on various image classification neural network models and datasets.

To the best of our knowledge, this study is the first to examine the effect that such properties have on the development of concept probing models, providing a starting point towards more research on how data affects concept probing, a topic that has been largely neglected [4]. We hope this work strengthens confidence in the reproducibility and reliability of concept probing, while providing evidence on how it is influenced by the quantity, provenance, and quality of the data, as well as the size of the probed model – helping to counter the spread of unverified folk theories about its applicability.

Acknowledgements

This work was supported by FCT I.P. through UID/04516/NOVA Laboratory for Computer Science and Informatics (NOVA LINC) and through PhD grant (DOI 10.54499/UI/BD/ 151266/2021), and by Project Sustainable Stone by Portugal - Valorization of Natural Stone for a digital, sustainable and qualified future, no 40, proposal C644943391-00000051, co-financed by PRR - Recovery and Resilience Plan of the European Union (Next Generation EU).

References

- [1] J. Adebayo, M. Muehly, I. Lliccardi, and B. Kim. Debugging Tests for Model Explanations. In *NeurIPS'20*, 2020.
- [2] G. Alain and Y. Bengio. Understanding intermediate layers using linear classifier probes. In *ICLR'17 Workshop Track*, 2017.
- [3] M. G. Augasta and T. Kathirvalavakumar. Reverse Engineering the Neural Networks for Rule Extraction in Classification Problems. *Neural Process. Lett.*, 35(2):131–150, 2012.
- [4] Y. Belinkov. Probing Classifiers: Promises, Shortcomings, and Advances. *Comput. Linguistics*, 48(1):207–219, 2022.
- [5] Y. Belinkov, N. Durrani, F. Dalvi, H. Sajjad, and J. R. Glass. What do Neural Machine Translation Models Learn about Morphology? In *ACL'17*, 2017.
- [6] E. Chu, D. Roy, and J. Andreas. Are Visual Explanations Useful? A Case Study in Model-in-the-Loop Prediction. abs/2007.12248, 2020.
- [7] J. Crabbé and M. van der Schaar. Concept activation regions: A generalized framework for concept-based explanations. In *NeurIPS'22*, 2022.
- [8] M. de Sousa Ribeiro, L. Krippahl, and J. Leite. Explainable Abstract Trains Dataset. *CoRR*, abs/2012.12115, 2020.
- [9] M. de Sousa Ribeiro, A. Leote, and J. Leite. CUB-200-2011 Attribute Revision, 2025. URL https://codelab.fct.unl.pt/di/is/neurosymb/cub_attr_rev.
- [10] M. de Sousa Ribeiro, A. Leote, and J. Leite. On the Performance of Concept Probing: The Influence of the Data. In *Procs. of ECAI'25*, 2025.
- [11] M. de Sousa Ribeiro, A. Leote, and J. Leite. Concept Probing: Where to Find Human-Defined Concepts. In *Procs. of NeSy'25*, 2025.
- [12] M. de Sousa Ribeiro, A. Leote, and J. Leite. GTSRB-Concepts: Additional German Traffic Sign Recognition Benchmark Labels and Ontology, 2025. URL https://codelab.fct.unl.pt/di/is/neurosymb/gtsrb_concepts.
- [13] M. de Sousa Ribeiro and J. Leite. Aligning Artificial Neural Networks and Ontologies towards Explainable AI. In *AAAI'21*, 2021.
- [14] J. Deng, W. Dong, R. Socher, L. Li, K. Li, and L. Fei-Fei. Imagenet: A large-scale hierarchical image database. In *CVPR'09*, 2009.
- [15] N. Durrani, H. Sajjad, F. Dalvi, and Y. Belinkov. Analyzing Individual Neurons in Pre-trained Language Models. In *EMNLP*, 2020.
- [16] J. Ferreira, M. de Sousa Ribeiro, R. Gonçalves, and J. Leite. Looking Inside the Black-Box: Logic-based Explanations for Neural Networks. In *KR'22*, 2022.
- [17] A. Ghorbani, J. Wexler, J. Y. Zou, and B. Kim. Towards Automatic Concept-based Explanations. In *NeurIPS'19*, 2019.
- [18] Y. Gong, G. Liu, Y. Xue, R. Li, and L. Meng. A survey on dataset quality in machine learning. *Inf. Softw. Technol.*, 162:107268, 2023.
- [19] W. Gurnee and M. Tegmark. Language Models Represent Space and Time. In *ICLR'24*, 2024.
- [20] G. V. Horn, O. M. Aodha, Y. Song, Y. Cui, C. Sun, A. Shepard, H. Adam, P. Perona, and S. J. Belongie. The INaturalist Species Classification and Detection Dataset. In *CVPR 2018*, 2018.
- [21] V. A. C. Horta, I. Tiddi, S. Little, and A. Mileo. Extracting knowledge from Deep Neural Networks through graph analysis. *Future Gener. Comput. Syst.*, 120:109–118, 2021.
- [22] D. Hupkes, S. Veldhoen, and W. H. Zuidema. Visualisation and 'Diagnostic Classifiers' Reveal How Recurrent and Recursive Neural Networks Process Hierarchical Structure. *J. Artif. Intell. Res.*, 61:907–926, 2018.
- [23] M. Ivanovs, R. Kadikis, and K. Ozols. Perturbation-based methods for explaining deep neural networks: A survey. *Pattern Recognit. Lett.*, 150:228–234, 2021.
- [24] G. Ke, Q. Meng, T. Finley, T. Wang, W. Chen, W. Ma, Q. Ye, and T. Liu. LightGBM: A Highly Efficient Gradient Boosting Decision Tree. In *NeurIPS'17*, 2017.
- [25] B. Kim, M. Wattenberg, J. Gilmer, C. J. Cai, J. Wexler, F. B. Viégas, and R. Sayres. Interpretability beyond feature attribution: Quantitative testing with concept activation vectors (TCAV). In *ICML'18*, 2018.
- [26] P. W. Koh, T. Nguyen, Y. S. Tang, S. Mussmann, E. Pierson, B. Kim, and P. Liang. Concept Bottleneck Models. In *Procs. of ICML'20*, 2020.
- [27] A. Krizhevsky. Learning Multiple Layers of Features from Tiny Images. 2009.
- [28] J. H. Lee, S. Lanza, and S. Wermter. From neural activations to concepts: A survey on explaining concepts in neural networks. *CoRR*, abs/2310.11884, 2023.
- [29] J. H. Lee, G. Mikriukov, G. Schwalbe, S. Wermter, and D. Wolter. Concept-based explanations in computer vision: Where are we and where could we go? *CoRR*, abs/2409.13456, 2024.
- [30] T. Linzen, E. Dupoux, and Y. Goldberg. Assessing the Ability of LSTMs to Learn Syntax-Sensitive Dependencies. *Trans. Assoc. Comput. Linguistics*, 4:521–535, 2016.
- [31] N. F. Liu, M. Gardner, Y. Belinkov, M. E. Peters, and N. A. Smith. Linguistic Knowledge and Transferability of Contextual Representations. In *NAACL-HLT'19*, 2019.
- [32] Z. Liu, P. Luo, S. Qiu, X. Wang, and X. Tang. Deepfashion: Powering robust clothes recognition and retrieval with rich annotations. In *CVPR'16*, 2016.
- [33] C. Lovering and E. Pavlick. Unit Testing for Concepts in Neural Networks. *Trans. Assoc. Comput. Linguistics*, 10:1193–1208, 2022.
- [34] J. Mu and J. Andreas. Compositional explanations of neurons. In *NeurIPS'20*, 2020.
- [35] C. G. Northcutt, L. Jiang, and I. L. Chuang. Confident Learning: Estimating Uncertainty in Dataset Labels. *J. Artif. Intell. Res.*, 70:1373–1411, 2021.
- [36] A. Pålsson and Y. Björnsson. Empirical Evaluation of Concept Probing for Game-Playing Agents. In *ECAI'24*, 2024.
- [37] T. Pimentel, N. Saphra, A. Williams, and R. Cotterell. Pareto Probing: Trading Off Accuracy for Complexity. In *EMNLP'20*, 2020.
- [38] T. Pimentel, J. Valvoda, R. H. Maudslay, R. Zmigrod, A. Williams, and R. Cotterell. Information-Theoretic Probing for Linguistic Structure. In *ACL'20*, 2020.
- [39] E. Poeta, G. Ciravegna, E. Pastor, T. Cerquitelli, and E. Baralis. Concept-based explainable artificial intelligence: A survey. *CoRR*, abs/2312.12936, 2023.
- [40] S. Rebuffi, R. Fong, X. Ji, and A. Vedaldi. There and Back Again: Revisiting Backpropagation Saliency Methods. In *CVPR*, 2020.
- [41] M. T. Ribeiro, S. Singh, and C. Guestrin. "Why Should I Trust You?": Explaining the Predictions of Any Classifier. In *SIGKDD'16*, 2016.
- [42] O. Russakovsky and L. Fei-Fei. Attribute learning in large-scale datasets. In *ECCV'10 Trends and Topics in Computer Vision Workshops*, 2010.
- [43] M. Sandler, A. G. Howard, M. Zhu, A. Zhmoginov, and L. Chen. MobileNetV2: Inverted Residuals and Linear Bottlenecks. In *CVPR'18*, 2018.
- [44] V. Sanh and A. M. Rush. Low-Complexity Probing via Finding Subnetworks. In *NAACL-HLT'21*, 2021.
- [45] L. Schmarje, V. Grossmann, C. Zelenka, S. Dippel, R. Kiko, M. Oszust, M. Pastell, J. Stracke, A. Valros, N. Volkmann, and R. Koch. Is one annotation enough? - A data-centric image classification benchmark for noisy and ambiguous label estimation. In *NeurIPS'22*, 2022.
- [46] G. P. J. Schmitz, C. Aldrich, and F. S. Gouw. ANN-DT: an algorithm for extraction of decision trees from artificial neural networks. *IEEE Trans. Neural Networks*, 10(6):1392–1401, 1999.
- [47] G. Schwalbe and B. Finzel. A comprehensive taxonomy for explainable artificial intelligence: a systematic survey of surveys on methods and concepts. *Data Min. Knowl. Discov.*, 38(5):3043–3101, 2024.
- [48] H. Shen and T. K. Huang. How Useful Are the Machine-Generated Interpretations to General Users? A Human Evaluation on Guessing the Incorrectly Predicted Labels. In *HCOMP'20*, 2020.
- [49] K. Simonyan and A. Zisserman. Very Deep Convolutional Networks for Large-Scale Image Recognition. In *ICLR'15*, 2015.
- [50] H. Song, M. Kim, and J. Lee. Toward robustness in multi-label classification: A data augmentation strategy against imbalance and noise. In

AAAI'24, 2024.

- [51] J. Stallkamp, M. Schlipsing, J. Salmen, and C. Igel. The German Traffic Sign Recognition Benchmark: A multi-class classification competition. In *IJCNN'11*, 2011.
- [52] M. Sundararajan, A. Taly, and Q. Yan. Axiomatic Attribution for Deep Networks. In *ICML'17*, 2017.
- [53] M. R. Taesiri, G. Nguyen, and A. Nguyen. Visual correspondence-based explanations improve AI robustness and human-AI team accuracy. In *NeurIPS'22*, 2022.
- [54] I. Tenney, P. Xia, B. Chen, A. Wang, A. Poliak, R. T. McCoy, N. Kim, B. V. Durme, S. R. Bowman, D. Das, and E. Pavlick. What do you learn from context? probing for sentence structure in contextualized word representations. In *ICLR'19*, 2019.
- [55] M. Tucker, P. Qian, and R. Levy. What if This Modified That? Syntactic Interventions with Counterfactual Embeddings. In *ACL/IJCNLP'21*, 2021.
- [56] United Nations. Vienna Convention on Road Traffic. United Nations Publications, 1968.
- [57] P. Villalobos, J. Sevilla, T. Besiroglu, L. Heim, A. Ho, and M. Hobbhahn. Machine Learning Model Sizes and the Parameter Gap. *CoRR*, abs/2207.02852, 2022.
- [58] C. Wah, S. Branson, P. Welinder, P. Perona, and S. Belongie. The Caltech-UCSD Birds-200-2011 Dataset. Technical Report CNS-TR-2011-001, 2011.
- [59] Y. Wang and S. H. Chung. Artificial intelligence in safety-critical systems: a systematic review. *Ind. Manag. Data Syst.*, 122(2):442–470, 2022.
- [60] WhatBird. Whatbird: Field guide to birds of north america. <http://www.whatbird.com>, 2022.
- [61] B. Wu, C. Xu, X. Dai, A. Wan, P. Zhang, M. Tomizuka, K. Keutzer, and P. Vajda. Visual transformers: Token-based image representation and processing for computer vision. abs/2006.03677, 2020.
- [62] H. Yu and S. Winkler. Image complexity and spatial information. In *QoMEX'12*, 2013.
- [63] X. Zhao, Y. Yang, F. Zhou, X. Tan, Y. Yuan, Y. Bao, and Y. Wu. Recognizing Part Attributes With Insufficient Data. In *ICCV*, 2019.
- [64] B. Zhou, À. Lapedriza, A. Khosla, A. Oliva, and A. Torralba. Places: A 10 million image database for scene recognition. *IEEE Trans. Pattern Anal. Mach. Intell.*, 40(6):1452–1464, 2018.
- [65] Y. Zhou and V. Srikumar. DirectProbe: Studying Representations without Classifiers. In *NAACL-HLT'21*, 2021.

A Additional Caltech-UCSD Birds-200-2011 Labels

In this Appendix, we describe the procedure used to relabel a subset of the Caltech-UCSD Birds-200-2011 dataset (CUB) [58] attributes.

As mentioned in [63, 26] some of the attributes in this dataset were found to be noisily labeled, which prompted us to perform a relabeling of the attribute labels involved in this work in order to guarantee the quality of the data used throughout the experiments.

From the 312 attributes in this dataset, a random subset of 11 attributes was considered: \exists hasBillShape.Needle, \exists hasBillShape.HookedSeabird, \exists hasHeadPattern.Striped, \exists hasBreastColor.Yellow, \exists hasThroatColor.Red, \exists hasEyeColor.Red, \exists hasBellyColor.Blue, \exists hasBellyColor.Yellow, \exists hasShape.DuckLike, \exists hasCrownColor.White, \exists hasCrownColor.Red.

These labels are made available in [9].

A.1 Relabeling Procedure

For each of the 11 selected attributes, the following procedure was performed:

1. Split the data into train and test images, according to the splits defined in the dataset.
2. For each of the train and test sets:
 - (a) Split the data into a positive set (P), where the attribute is present, and a negative set (N), where the attribute is absent, of samples, according to the original labels in the dataset.
 - (b) Define a constant $n = \min(\{|P|, |N|, 500\})$
 - (c) Randomly select n samples from P :
 - i. Relabel the selected samples.
 - (d) Randomly select n samples from N :
 - i. Relabel the selected samples.

This procedure produces a new set of labels for a subset of samples of the original dataset, for a given attribute.

The relabeling of each image was performed according to the descriptions provided in the field guide [60] referred in [58]. The relabeling of the attributes was made with respect to whether the attributes were visible in each image. Thus, even if a bird of a given species is known to have a certain attribute, but it is not visible in the image, the attribute is labeled as being absent from the image.

A.2 Label Statistics

The distribution of positive and negative samples in the original labels is shown in Table A.1. Table A.2 shows the resulting number of samples for each attribute after executing the described procedure. Table A.3 summarizes the identified discrepancies – instances originally labeled as positive but found to be negative, and instances labeled as negative but found to be positive.

A.3 Examples of Attribute Labeling Discrepancies

Figure A.1 shows instances for each attribute, illustrating three cases: i) correctly labeled samples where the attribute is present; ii) mislabeled samples where the attribute is absent but originally labeled as present; iii) and mislabeled samples where the attribute is present but originally labeled as absent.

Attribute	# Original Positive	# Original Negative
\exists hasBillShape.Needle	289	11499
\exists hasBillShape.HookedSeabird	751	11037
\exists hasHeadPattern.Striped	805	10983
\exists hasBreastColor.Yellow	1613	10175
\exists hasThroatColor.Red	453	11335
\exists hasEyeColor.Red	278	11510
\exists hasBellyColor.Blue	271	11517
\exists hasBellyColor.Yellow	1692	10096
\exists hasShape.DuckLike	723	11065
\exists hasCrownColor.White	1433	10355
\exists hasCrownColor.Red	572	11216

Table A.1. Number of samples for each attribute in the original dataset.

Attribute	# Relabeled Positive	# Relabeled Negative
\exists hasBillShape.Needle	190	414
\exists hasBillShape.HookedSeabird	629	875
\exists hasHeadPattern.Striped	324	675
\exists hasBreastColor.Yellow	387	642
\exists hasThroatColor.Red	304	678
\exists hasEyeColor.Red	208	382
\exists hasBellyColor.Blue	141	436
\exists hasBellyColor.Yellow	371	639
\exists hasShape.DuckLike	502	922
\exists hasCrownColor.White	245	760
\exists hasCrownColor.Red	401	785

Table A.2. Number of samples for each attribute after executing the relabeling procedure.

Attribute	# Mislabeled Positive	# Mislabeled Negative
\exists hasBillShape.Needle	99	0
\exists hasBillShape.HookedSeabird	153	31
\exists hasHeadPattern.Striped	234	59
\exists hasBreastColor.Yellow	137	6
\exists hasThroatColor.Red	151	2
\exists hasEyeColor.Red	78	8
\exists hasBellyColor.Blue	130	0
\exists hasBellyColor.Yellow	151	15
\exists hasShape.DuckLike	239	18
\exists hasCrownColor.White	259	4
\exists hasCrownColor.Red	177	6

Table A.3. Number of instances originally labeled as positive but found to be negative (# Mislabeled Positive), and instances labeled as negative but found to be positive (# Mislabeled Negative), for each attribute.


Attribute Name	Correct Positive			Mislabel Positive			Mislabel Negative		
\exists hasBillShape.Needle									
\exists hasBillShape.HookedSeabird									
\exists hasHeadPattern.Striped									
\exists hasBreastColor.Yellow									
\exists hasThroatColor.Red									
\exists hasEyeColor.Red									
\exists hasBellyColor.Blue									
\exists hasBellyColor.Yellow									
\exists hasShape.DuckLike									
\exists hasCrownColor.White									
\exists hasCrownColor.Red									

Figure A.1. Instances of correctly labeled samples and mislabeled samples.

B Additional German Traffic Sign Recognition Benchmark Labels and Ontology

In this Appendix, we describe the procedure used to label a subset of the German Traffic Sign Recognition Benchmark dataset (GTSRB) [51] regarding additional concepts of interest defined in the 1968 Convention on Road Signs and Signals [56], which describes each type of traffic sign in the dataset based on visual features.

These labels and ontology are made available in [12].

B.1 Ontology Development

This ontology was obtained by translating to Description Logics all of the excerpts related to the 43 traffic signs included in the GTSRB dataset from the 1968 Convention on Road Signs and Signals [56].

The ontology was designed by identifying concepts and roles, and forming axioms that reflect as close as possible the descriptions provided in [56] regarding the traffic signs considered in the GTSRB dataset. Additionally, axioms reflecting the hierarchies and categories of the traffic signs in the GTSRB dataset, were defined based on the descriptions in [56].

This process resulted in an ontology that describes the 43 signs existing in the GTSRB dataset, and how they relate to the 4 traffic signal categories, based on the following vocabulary:

- Shape – a sign may have a triangular, circular, rectangular, octagonal, or diamond shape;
- Ground – a sign may have a white, yellow, blue, red, or orange ground;
- Border – a sign may have a white, red, or black border;
- Bar – a sign may have a white or black bar;
- Symbol – a sign may have symbols; 35 different symbols were considered.

Three different kinds of information were provided in [56] regarding the traffic signals and their hierarchy:

- Information describing the features of a given traffic signal, e.g., the following excerpt provides information regarding the features of a ‘Model B, 2a Stop sign’:
“Model B, 2a is octagonal with a red ground bearing the word "STOP" in white in English or in the language of the State concerned;”, which resulted in the axiom:
 $\exists \text{hasShape.Octagon} \sqcap \exists \text{hasGround.Red} \sqcap \exists \text{hasSymbol.}(\text{White} \sqcap \text{Stop}) \equiv \text{B2a}$.
- Information describing which traffic signals belong to a given traffic signal class, e.g., the following excerpt provides information regarding which traffic signs belong to the class ‘A.1. Danger Warning signs’:
“Section A DANGER WARNING SIGNS (...) 1. Dangerous bend or bends:
Warning of a dangerous bend or succession of dangerous bends shall be given by one of the following symbols, whichever is appropriate:
(a) A, 1^a: left bend
(b) A, 1^b: right bend
(c) A, 1^c: double bend, or succession of more than two bends, the first to the left
(d) A, 1^d: double bend, or succession of more than two bends, the first to the right.”

which resulted in the following axiom: $\text{A1a} \sqcup \text{A1b} \sqcup \text{A1c} \sqcup \text{A1d} \sqsubseteq \text{A1}$;

- Information describing how different classes of traffic signals are categorized, e.g., the following excerpt provides information regarding which traffic signs classes belong to the category ‘A. Danger warning signs’:

“The “A” DANGER WARNING signs shall be of model A^a or model A^b both described here and reproduced in Annex 3, except signs A, 28 and A, 29 described in paragraphs 28 and 29 below respectively.”, which resulted in the axiom: $\text{A}^a \sqcup \text{A}^b \sqcup \text{A28} \sqcup \text{A29} \equiv \text{A}$;

To ensure that the ontology properly describes all traffic signals existing in the GTSRB dataset, we added the descriptions of traffic signs that were introduced after the 1968 Convention on Road Signs and Signals, such as the signs: A 33, A 34, and C 3^{e3}.

The concept Pole, representing a traffic signal’s pole was also added to the ontology. This non-relevant concept is not involved in any of the ontology’s axioms, or even directly involved in the task performed by the main network f_{GTSRB} .

The complete ontology can be found in Figure B.1.

B.2 Labeling Procedure

From the resulting ontology the following 41 of interest were considered for labeling: $\exists \text{hasBar.T}$, $\exists \text{hasBar.Black}$, $\exists \text{hasBar.White}$, $\exists \text{hasBorder.T}$, $\exists \text{hasBorder.Black}$, $\exists \text{hasBorder.Red}$, $\exists \text{hasBorder.White}$, $\exists \text{hasGround.Red}$, $\exists \text{hasGround.}(\text{White} \sqcup \text{Yellow})$, $\exists \text{hasGround.Yellow}$, StartProhibition , EndProhibition , $\exists \text{hasShape.Circle}$, $\exists \text{hasShape.Diamond}$, $\exists \text{hasShape.Triangle}$, $\exists \text{hasShape.Octagon}$, $\exists \text{hasSymbol.T}$, $\exists \text{hasSymbol.Black}$, $\exists \text{hasSymbol.White}$, $\exists \text{hasSymbol.NoEntryGoods}$, $\exists \text{hasSymbol.Overtaking}$, $\exists \text{hasSymbol.OvertakingGoods}$, $\exists \text{hasSymbol.Speed20}$, $\exists \text{hasSymbol.Speed30}$, $\exists \text{hasSymbol.Speed50}$, $\exists \text{hasSymbol.Speed60}$, $\exists \text{hasSymbol.Speed70}$, $\exists \text{hasSymbol.Speed80}$, $\exists \text{hasSymbol.Speed100}$, $\exists \text{hasSymbol.Speed120}$, $\exists \text{hasSymbol.Stop}$, D1a1, D1a4, D1a5, D1a6, D1a7, D2a1, D2a2, D3, Blue, Pole.

For each of these concepts, a random subset of 200 samples from each of the 43 traffic sign classes contained in the training set of GTSRB was manually labeled. Similarly, for testing purposes, a random subset of 60 images from each of the 43 traffic sign classes was labeled.

The resulting distribution of positive and negative samples in the train and test sets of the GTSRB dataset is shown in Table B.1.

Figure B.2 shows random instances of samples where the considered concepts was present (positive samples) and absent (negative samples).

$A^a \sqcup A^b \sqcup A28 \sqcup A29 \equiv A$
 $\exists \text{hasShape.Triangle} \sqcap \exists \text{hasGround. (White} \sqcup \text{Yellow)} \sqcap \exists \text{hasBorder.Red} \sqcap \exists \text{hasSymbol.T} \equiv A^a$
 $A1 \sqcup A4 \sqcup A7 \sqcup A9 \sqcup A13 \sqcup A14 \sqcup A15 \sqcup A16 \sqcup A17 \sqcup A19 \sqcup A32 \sqcup A33 \sqcup A34 \sqsubseteq A$
 $A4b2 \sqsubseteq A4 \quad A7a \sqsubseteq A7 \quad A15b \sqsubseteq A15 \quad A17a \sqsubseteq A17 \quad A19a \sqsubseteq A19$
 $A1a \sqcup A1b \sqcup A1c \sqsubseteq A1$
 $A \sqcap \exists \text{hasSymbol.SingleLeftBend} \equiv A1a$
 $A \sqcap \exists \text{hasSymbol.SingleRightBend} \equiv A1b$
 $A \sqcap \exists \text{hasSymbol.TwoOrMoreLeftBend} \equiv A1c$
 $A \sqcap \exists \text{hasSymbol.RightNarrow} \equiv A4b2$
 $A \sqcap \exists \text{hasSymbol.RoadDeformities} \equiv A7a$
 $A \sqcap \exists \text{hasSymbol.SlipperyRoad} \equiv A9$
 $A \sqcap \exists \text{hasSymbol.Children} \equiv A13$
 $A \sqcap \exists \text{hasSymbol.Cyclists} \equiv A14$
 $A \sqcap \exists \text{hasSymbol.WildAnimals} \equiv A15b$
 $A \sqcap \exists \text{hasSymbol.RoadWorks} \equiv A16$
 $A \sqcap \exists \text{hasSymbol.VerticalLightSignals} \equiv A17a$
 $A \sqcap \exists \text{hasSymbol.IntersectionPriority} \equiv A19a$
 $A \sqcap \exists \text{hasSymbol.Danger} \equiv A32$
 $A \sqcap \exists \text{hasSymbol.Pedestrians} \equiv A33$
 $A \sqcap \exists \text{hasSymbol.IceSnow} \equiv A34$

$B1 \sqcup B2 \sqcup B3 \sqsubseteq B$
 $B2a \sqcup B2b \equiv B2$
 $\exists \text{hasShape.Triangle} \sqcap \exists \text{hasGround. (White} \sqcup \text{Yellow)} \sqcap \exists \text{hasBorder.Red} \sqcap \neg \exists \text{hasSymbol.T} \equiv B1$
 $\exists \text{hasShape.Octagon} \sqcap \exists \text{hasGround.Red} \sqcap \exists \text{hasSymbol. (White} \sqcap \text{Stop)} \equiv B2a$
 $\exists \text{hasShape.Diamond} \sqcap \exists \text{hasGround. (Yellow} \sqcup \text{Orange)} \sqcap \exists \text{hasBorder.White} \equiv B3$

$C \sqsubseteq \exists \text{hasShape.Circle}$
 $\text{StartProhibition} \sqsubseteq (\exists \text{hasGround. (White} \sqcup \text{Yellow)} \sqcup (\exists \text{hasGround.Blue} \sqcap \exists \text{hasBorder.Red})) \sqcap$
 $\forall \text{hasSymbol. (Black} \sqcup \text{Red)} \sqcap \forall \text{hasBar. (Red} \sqcup \text{White)}$
 $C1 \sqcup C2 \sqcup C3 \sqcup C13 \sqcup C14 \sqcup C17 \sqsubseteq C$
 $C1a \sqsubseteq C1$
 $C3e3 \sqsubseteq C3$
 $C13aa \sqcup C13bb \sqsubseteq C13$
 $C14_20 \sqcup C14_30 \sqcup C14_50 \sqcup C14_60 \sqcup C14_70 \sqcup C14_80 \sqcup C14_100 \sqcup C14_120 \sqsubseteq C14$
 $C17a \sqcup C17b_80 \sqcup C17c \sqcup C17d \sqsubseteq C17$
 $\exists \text{hasShape.Circle} \sqcap \exists \text{hasGround.Red} \sqcap \neg \exists \text{hasSymbol.T} \sqcap \exists \text{hasBar.White} \equiv C1a$
 $\exists \text{hasShape.Circle} \sqcap \exists \text{hasGround. (White} \sqcup \text{Yellow)} \sqcap \exists \text{hasBorder.Red} \sqcap \neg \exists \text{hasSymbol.T} \equiv C2$
 $\text{StartProhibition} \sqcap \exists \text{hasSymbol.NoEntryGoods} \sqcap \neg \exists \text{hasBar.T} \equiv C3e3$
 $\text{StartProhibition} \sqcap \exists \text{hasSymbol.Overtaking} \sqcap \neg \exists \text{hasBar.T} \equiv C13aa$
 $\text{StartProhibition} \sqcap \exists \text{hasSymbol.OvertakingGoods} \sqcap \neg \exists \text{hasBar.T} \equiv C13bb$
 $\text{StartProhibition} \sqcap \exists \text{hasSymbol.Speed20} \equiv C14_20$
 $\text{StartProhibition} \sqcap \exists \text{hasSymbol.Speed30} \equiv C14_30$
 $\text{StartProhibition} \sqcap \exists \text{hasSymbol.Speed50} \equiv C14_50$
 $\text{StartProhibition} \sqcap \exists \text{hasSymbol.Speed60} \equiv C14_60$
 $\text{StartProhibition} \sqcap \exists \text{hasSymbol.Speed70} \equiv C14_70$
 $\text{StartProhibition} \sqcap \exists \text{hasSymbol.Speed80} \equiv C14_80$
 $\text{StartProhibition} \sqcap \exists \text{hasSymbol.Speed100} \equiv C14_100$
 $\text{StartProhibition} \sqcap \exists \text{hasSymbol.Speed120} \equiv C14_120$
 $\exists \text{hasShape.Circle} \sqcap \exists \text{hasGround. (White} \sqcup \text{Yellow)} \sqcap$
 $\neg \exists \text{hasBorder.T} \sqcap \exists \text{hasBar.Black} \sqcap \neg \exists \text{hasSymbol.T} \equiv C17a$
 $\exists \text{hasShape.Circle} \sqcap \exists \text{hasGround. (White} \sqcup \text{Yellow)} \sqcap$
 $\neg \exists \text{hasBorder.T} \sqcap \exists \text{hasBar.Black} \sqcap \exists \text{hasSymbol.Speed80} \equiv C17b_80$
 $\exists \text{hasShape.Circle} \sqcap \exists \text{hasGround. (White} \sqcup \text{Yellow)} \sqcap$
 $\neg \exists \text{hasBorder.T} \sqcap \exists \text{hasBar.Black} \sqcap \exists \text{hasSymbol.Overtaking} \equiv C17c$
 $\exists \text{hasShape.Circle} \sqcap \exists \text{hasGround. (White} \sqcup \text{Yellow)} \sqcap$
 $\neg \exists \text{hasBorder.T} \sqcap \exists \text{hasBar.Black} \sqcap \exists \text{hasSymbol.OvertakingGoods} \equiv C17d$

$D \sqsubseteq \exists \text{hasShape. (Circle} \sqcup \text{Rectangle)}$
 $D \sqsubseteq (\exists \text{hasGround.Blue} \sqcap \exists \text{hasSymbol.White}) \sqcup (\exists \text{hasGround.White} \sqcap \exists \text{hasSymbol.Black})$
 $D1 \sqcup D2 \sqcup D3 \sqsubseteq D$
 $D1a1 \sqcup D1a2 \sqcup D1a3 \sqcup D1a6 \sqcup D1a7 \sqsubseteq D1$
 $D2a1 \sqcup D2a2 \sqsubseteq D2$
 $D \sqcap \exists \text{hasSymbol.DirectionStraight} \equiv D1a1$
 $D \sqcap \exists \text{hasSymbol.DirectionLeft} \equiv D1a2$
 $D \sqcap \exists \text{hasSymbol.DirectionRight} \equiv D1a3$
 $D \sqcap \exists \text{hasSymbol.DirectionLeftStraight} \equiv D1a6$
 $D \sqcap \exists \text{hasSymbol.DirectionRightStraight} \equiv D1a7$
 $D \sqcap \exists \text{hasSymbol.PassLeft} \equiv D2a1$
 $D \sqcap \exists \text{hasSymbol.PassRight} \equiv D2a2$
 $D \sqcap \exists \text{hasSymbol.Roundabout} \equiv D3$

Figure B.1. Resulting ontology describing the GTSRB domain.

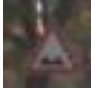



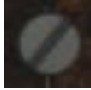

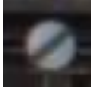
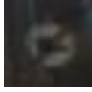
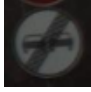



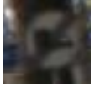
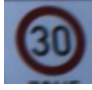
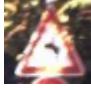






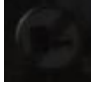
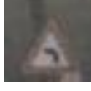

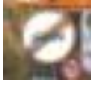

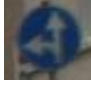








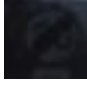



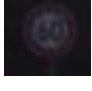






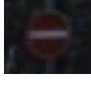

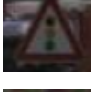
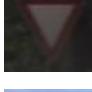


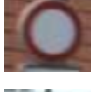
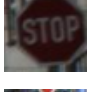






Concept Name	Positive Samples			Negative Samples		
$\exists \text{hasSymbol.T}$						
$\exists \text{hasBar.Black}$						
$\exists \text{hasSymbol.Black}$						
Blue						
$\exists \text{hasShape.Circular}$						
Pole						
$\exists \text{hasGround.Red}$						
$\exists \text{hasSymbol.Speed80}$						
$\exists \text{hasShape.Triangular}$						
$\exists \text{hasGround.White}$						

Figure B.2. Positive and negative samples for each concept.

Concept	Train		Test	
	# Positive Samples	# Negative Samples	# Positive Samples	# Negative Samples
\exists hasBar. T	1178	7422	350	2230
\exists hasBar.Black	870	7730	251	2329
\exists hasBar.White	309	8291	92	2488
\exists hasBorder. T	5832	2768	1761	819
\exists hasBorder.Black	1018	7582	359	2221
\exists hasBorder.Red	4710	3890	1367	1213
\exists hasBorder.White	202	8398	57	2523
\exists hasGround.Red	377	8223	109	2471
\exists hasGround.(White \sqcup Yellow)	6451	2149	1941	639
\exists hasGround.Yellow	262	8338	72	2508
StartProhibition	2660	5940	795	1785
EndProhibition	810	7790	240	2340
\exists hasShape.Circle	5058	3542	1524	1056
\exists hasShape.Diamond	202	8398	60	2520
\exists hasShape.Triangle	3313	5287	999	1581
\exists hasShape.Octagon	200	8400	60	2520
\exists hasSymbol. T	7612	988	2290	290
\exists hasSymbol.Black	5611	2989	1696	884
\exists hasSymbol.White	1820	6780	544	2036
\exists hasSymbol.NoEntryGoods	166	8434	51	2529
\exists hasSymbol.Overtaking	306	8294	97	2483
\exists hasSymbol.OvertakingGoods	310	8290	86	2494
\exists hasSymbol.Speed20	196	8404	60	2520
\exists hasSymbol.Speed30	186	8414	59	2521
\exists hasSymbol.Speed50	178	8422	54	2526
\exists hasSymbol.Speed60	180	8420	57	2523
\exists hasSymbol.Speed70	188	8412	60	2520
\exists hasSymbol.Speed80	348	8252	102	2478
\exists hasSymbol.Speed100	164	8436	58	2522
\exists hasSymbol.Speed120	146	8454	43	2537
\exists hasSymbol.Stop	196	8404	58	2522
D1a1	200	8400	60	2520
D1a4	200	8400	60	2520
D1a5	200	8400	60	2520
D1a6	200	8400	60	2520
D1a7	200	8400	60	2520
D2a1	200	8400	60	2520
D2a2	200	8400	60	2520
D3	200	8400	60	2520
Blue	2138	6462	686	1894
Pole	3413	5187	863	1717

Table B.1. Number of samples for each labeled concept of interest in the dataset.